SP2016_*3124815*

SPACE PROPULSION 2016

OPTICAL INVESTIGATION OF THE LOX-JET DISINTEGRATION PROCESSES AT HIGH PRESSURE CONDITIONS IN A LOX/H2 SINGLE COAXIAL INJECTOR COMBUSTION CHAMBER

D. I. Suslov, J. Hardi, B. Knapp, M. Oschwald

Institute of Space Propulsion, Germany Aerospace Center (DLR)

74219 Lampoldshausen, Germany

dmitry.suslov@dlr.de; justin.hardi@dlr.de; bernhard.knapp@dlr.de; michael.oschwald@dlr.de

KEYWORDS: combustion chamber, high pressure combustion, LOX-core, shadowgraph

ABSTRACT:

Injector behavior is of utmost importance for the performance and stability of liquid rocket engines. A major challenge is achieving a highly efficient homogeneous mixture and effective chemical reaction of fuels at minimum chamber length. Despite substantial progress in numerical simulations a need for experimental data at representative conditions for development and validation of numerical design tools still exists. Therefore, in the framework of the DLR-project "ProTau", we have performed tests to create an extended data base for numerical tool validation for high pressure LOX/H2 combustion.

During the experimental investigations a windowed DLR subscale thrust chamber model "C" (designated BKC) has been operated over a broad range of conditions at reduced pressures of approximately 0.8 (P_{CC} = 4 MPa), 1 (P_{CC} = 5 MPa) and 1.2 (P_{CC} = 6 MPa) with respect to the thermodynamic critical pressure of oxygen. Liquid oxygen and gaseous hydrogen have been injected through a single coaxial injector element at temperatures of ca. 120 K and ca. 130 K, respectively. High-speed optical diagnostics have been implemented, including imaging of OH* emission and shadowgraph imaging at frequencies from 8 kHz up to 10 kHz to visualize the flow field

NOMENCLATURE:

J	momentum flux ratio $J= \rho_{GH2}V^2_{GH2}/\rho_{LOX}V^2_{LOX}$
LOX	liquid oxygen
LRE	liquid rocket engine
P_{CC}	combustion chamber pressure
$P_{crit,O2}$	oxygen critic pressure
ROF	oxygen to fuel ratio
Pr	reduced pressure, $Pr= P_{CC}/P_{crit,O2}$
VR	velocity ratio, $VR= V_{GH2}/V_{LOX}$
V_{GH2}	hydrogen injection velocity
V_{LOX}	oxygen injection velocity

1. INTRODUCTION

In the development of modern liquid rocket engines (LRE), injector head design is of the utmost importance for performance and combustion stability. Optimized designs must show high combustion efficiency in combination with low

pressure drop across the injector at minimum chamber length and low manufacturing costs.

Modern LREs operated with liquid oxygen and hydrogen (LOX/H2) like the Space Shuttle Main Engine (SSME), RD-0120 and the Ariane 5 Vulcain II engine are equipped with classical shear-coaxial injector elements. While LOX is fed through the central tube at about 20-30 m/s, hydrogen is delivered through a circumferential passage at high velocities of about 200-300 m/s. The atomization und the mixing processes are driven by LOX jet disintegration due to shear forces. Coaxial injectors provide a uniform initial distribution of the liquid oxygen and adequate mixing characteristics and show sufficient overall performance and stable operation.

The research activities of the last few years on LOX/H2 have provided an improved understanding of the injection und combustion processes in LREs. But many thermo- and fluid dynamic effects on highly turbulent, reactive flow fields at elevated pressure remain widely unknown.

Today, the development of new rocket propulsion occurs during an era of significantly reduced R&D budgets. However the capabilities of computational systems are growing rapidly. Consequently, the main focus in development of new concepts, or upgrades to previous designs, has been shifting more and more from the paradigm of the 1950s-1960s of full-scale hot fire testing to numerical modelling and simulation.

Despite substantial progress in numerical modelling, a need for experimental data at representative conditions for the development and validation of numerical design tools still exists. Thorough validation of numerical models requires not only experimentally determined global parameters such as combustion chamber pressure and mass flow rates, but also highly detailed and precise information concerning the flow parameters as well as impeccable knowledge of the boundary conditions during the test. Realising these requirements often leads to “partial modelling” by reference experiments, to investigate selected phenomena and deliberately ignoring some of the similarity requirements, depending upon the problem at hand. To help bridge such data sets with reality, windowed combustion chambers with single coaxial injector have sometimes been used for intra-chamber injection and combustion studies by providing optical access for the application of optical diagnostics parallel to conventional measurement of global parameters.

One such windowed combustion chamber is the model ‘C’, referred to as BKC, operated at DLR Lampoldshausen. This paper presents preliminary analysis from this data set, which is anticipated will assist in providing a comprehensive quantitative and qualitative basis for validation of numerical models and contribute to the understanding of high pressure combustion phenomena.

2. EXPERIMENTAL SETUP AND TEST PARAMETERS

The applied subscale combustion chamber and test bench have allowed an experimental investigation at real rocket engine like operating conditions. A test campaign with BKC was performed in the current work, with the aim of generating a comprehensive experimental database for operating conditions.

2.1. Test Bench

The investigations presented here were performed at the European Research and Technology Test Facility P8 (Figure 1). The P8 facility is a high-pressure test bench for subscale rocket trust chambers located at the Institute of Space Propulsion at DLR Lampoldshausen.

Figure 1: European Research and Technology Test Facility P8, DLR Lampoldshausen

This test facility enables investigations with the cryogenic propellants hydrogen, oxygen and natural gas at typical rocket engine operating conditions [1].

2.2. DLR Subscale Combustion Chamber Model "C"

The windowed combustion chamber has been specifically developed and manufactured for intra-chamber injection and combustion studies by providing optical access for the application of optical diagnostics.

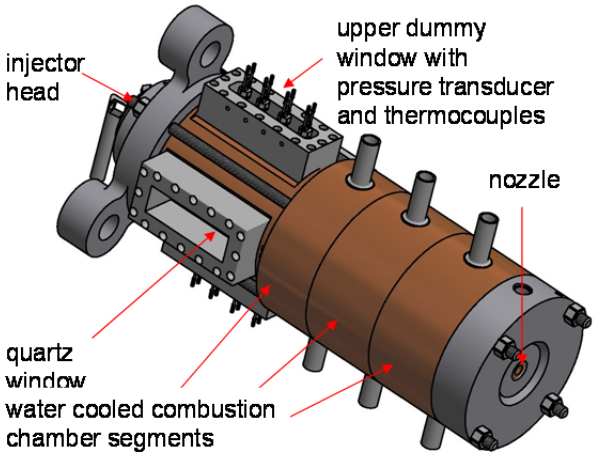

Figure 2: DLR subscale combustion chamber model "C" (BKC) with optical access

A sketch of the windowed combustion chamber is given in Figure 2. The combustion chamber can be operated at up to 7.0 MPa. The chamber is highly versatile with interchangeable nozzles and injector head configurations

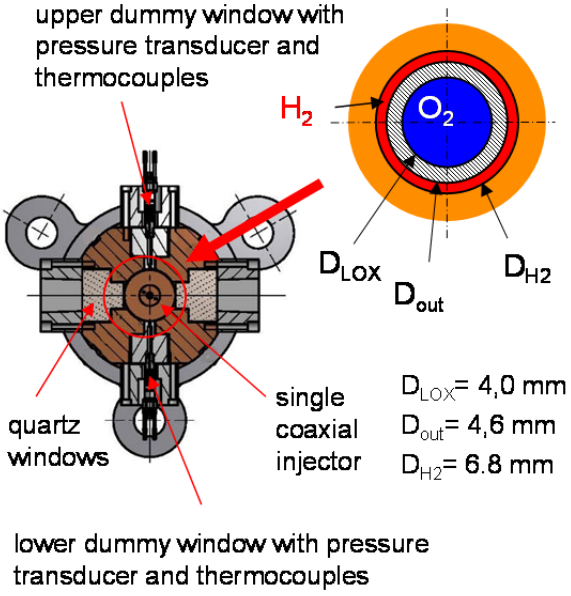

Figure 3: DLR subscale combustion chamber model "C" (BKC) cross section

The combustion chamber is segmented into four separate water-cooled sections and a nozzle. On these grounds the windowed section can be placed at various axial locations. This feature has been used to achieve optical access along the full combustion chamber length, 0 mm to 370 mm. This distance is close to the length of real rocket engines up to nozzle throat. A more detailed description of the different test configuration is presented in [9]. The inner diameter of the presented subscale combustion chamber is 50mm. Contraction ratio (ratio of the combustion chamber area to area of the nozzle throat) is 8.35.

2.3. Operation Conditions

A well-established operating sequence has been used to provide steady state conditions at three relevant pressure levels including sub-, near- and supercritical conditions with respect to the critical pressure of oxygen as seen in Figure 4 and Table 1. The start time (t= 0 s) accords to the combustion chamber ignition.

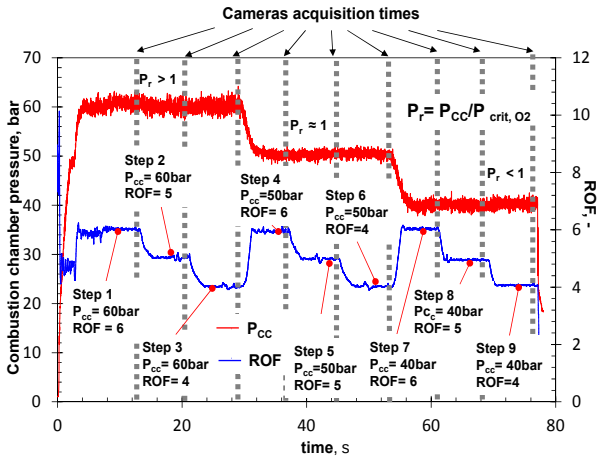

Figure 4: Test sequence

In this context the reduced pressure has been defined as: Pr= $P_{CC}/P_{crit,O2}$ Each pressure level includes three different ROF ranges of 6, 5, and 4.

The duration of each load step is 8 s, which allows a stable, steady-state thermal and flow condition to be reached. The last 1 s of each test condition (step) has been used for high speed optical imaging. The high precision regulation system and extensive experience of the test personnel provided superior repeatability of the test conditions (±2%), which is of great importance for a comparison test runs with different hardware configurations

Table 1: Preset operation conditions for tests on using rocket combustor "BKC".

Load step [-]	P_{CC} [bar]	$ROF_{Injector}$ [-]
1	62	6
2	61	5
3	61	4
4	51	6
5	50	5
6	50	4
7	40	6
8	40	5
9	40	4

The injection conditions for all load steps are shown in Table 2. The LOX and H2 injection temperatures have been held relatively constant at 120 K and 160 K, respectively. Liquid oxygen injection velocities of about 15-30 m/s and hydrogen velocities of about 350-440 m/s were of the same order of magnitude as those in comparable shear coaxial injector studies [2], [4]. The calculation of the injection velocities is based on the full injection area without consideration of the boundary layer displacement thickness.

Table 2: Measured injection conditions for tests on using rocket combustor "BKC".

Load step [-]	u_{LOX} [m/s]	u_{H2} [m/s]	VR [-]	J [-]
1	27.2	320	12	1.3
2	25.1	365	15	1.9
3	23.8	436	18	3.0
4	21.1	315	15	1.6
5	20.5	364	18	2.3
6	19.6	432	22	3.5
7	16.8	307	18	2.0
8	16.2	360	22	2.9
9	15.8	420	27	4.2

3. SETUP OF THE OPTICAL ACQUISITION SYSTEM

Two different camera systems were used to observe the influence of the propellant injection conditions on the flame behavior. All systems had to be specially protected to prevent potential damage by radiative heat transfer, vibrations or acoustic loads. A specific imaging setup was implemented to capture simultaneous OH emission and flow visualization with shadowgraph imaging using high-speed cameras. A schematic of the apparatus and a photograph in the test cell are shown in Figure 5.

The system used for shadowgraph imaging consists of an LED illuminator as a light source, a small aperture followed by an achromatic lens with a focal length of 1250 mm to perform a parallel light beam through the flow field normal to the plane viewing windows of the combustion chamber BKC.

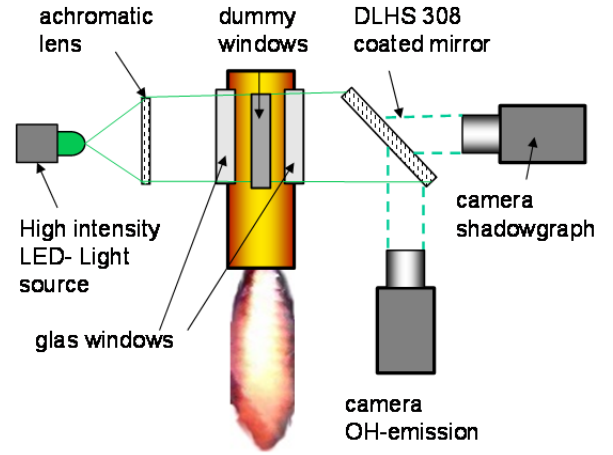

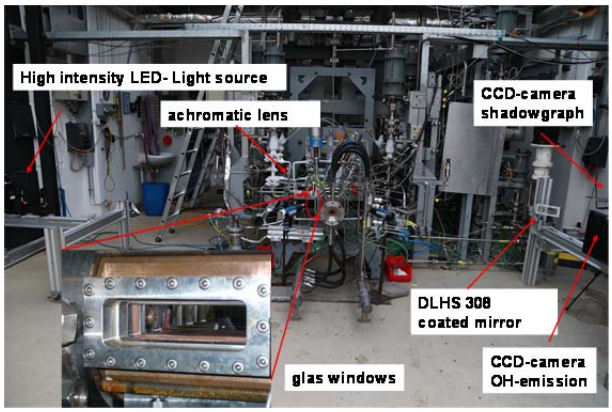

Figure 5: Schematic illustration and photograph of the optical diagnostic setup at the test facility P8

At the opposite side of the chamber a combination of two filters, a 300 mm camera lens, and a field aperture to reduce scattered light from the environment are located in front of the high speed camera at a distance behind the combustion chamber. The point shaped light source produces diverging light which is parallelized by the achromatic lens and is then transmitted through the combustion chamber windows. The camera lens focusses the parallel light back to the camera chip and the shadow picture produced by the

inhomogeneous density field is then recorded in the vertical plane of the camera chip.

The camera for acquisition of the shadowgraph images with a bit depth of 16 is a Photron Fastcam SA5. For background illumination a high-power-LED illuminator model IL-106G was used. This LED illuminator provides extremely bright and non-coherent continuous light with a central wavelength of around 528 nm. This LED lamp was used to provide an illumination source which exceeds the luminosity of the flame at this wavelength. Yellow GG495 filter and blue BG38 filters have been applied to together act as a band pass filter for the green LED light of the Illuminator.

OH* visualization has been carried out simultaneously with the shadowgraph imaging through a 310 nm deflective mirror. In order to look at the same point of interest in the flow field inside the combustion chamber with both shadowgraph and OH* cameras, this beam splitter has been mounted in the optical path between shadowgraph camera and combustion chamber window in a 45° orientation as can be seen in Figure 5.

4. RESULTS OF THE OPTICAL INVESTIGATIONS

The focus of the current investigation is to create database for verification of numerical tools. For this purpose the optical data have been combined with detailed measurement of the surface temperature and pressure distribution along the combustion chamber main axis that should serve to define boundary conditions for numerical simulation [9].The main objectives were the investigation of the flow characteristics, atomization and mixing processes by optical measurement methodologies.

Figure 6 shows compiled shadowgraph images over the full combustion chamber length at investigated load steps. The reference value x = 0 mm corresponds to the face plate of the injector

While at low combustion chamber pressure (Pr < 1, load steps 7-9) atomization of the LOX-core is completed at x = 280 mm, at higher thermal loads (Pr > 1, load steps 1-3) several dark LOX-spots are visible up to the end of the observation area. Because the main aim of the investigation is the creation of an extended data basis for numerical tool validation, the major goal of the test program was to maximize the range of flow conditions captured.

To reduce configuration change effort during the campaign, the contraction ratio of combustion chamber (BKC) was constant and different pressure was the result of different propellant mass flow rates. Therefore, a direct comparison of the flow condition at Pr > 1 and at Pr < 1 has very limited relevance and is not presented in this paper.

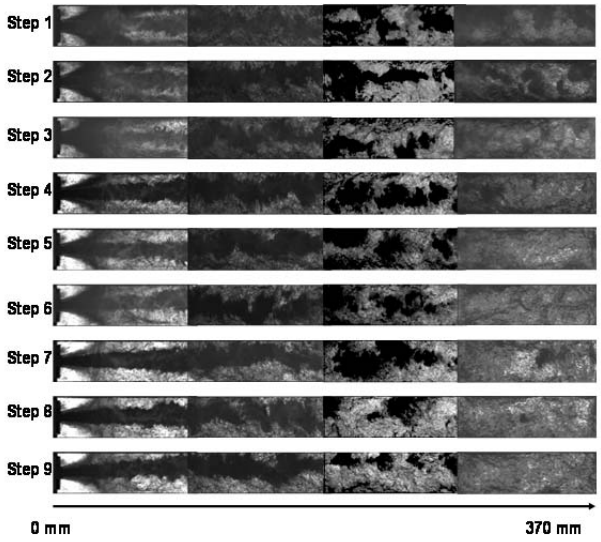

Figure 6: Compiled shadowgraph images at different load steps

The analysis of the LOX-core is hindered by high variation in the absorption coefficient of the dense gas in the combustion chamber, as well as condensation of the combustion products. To simplify comparison between configurations and operating steps, the shadowgraph images have been converted to the binary (black and white) pictures. (Figure 7, gradient recognition).

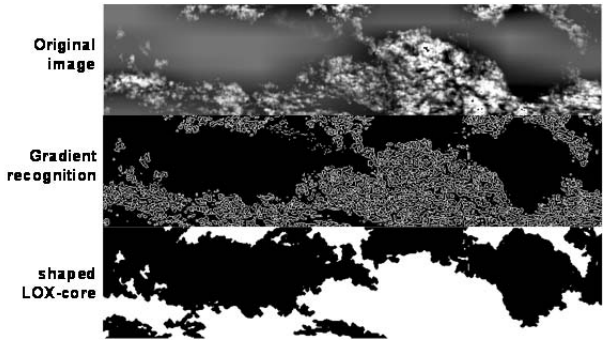

Figure 7: Handling steps at processing of the shadowgraph images

The image intensity and texture has been taken into consideration in this process. The area with high local variation of the gradients has been classed as background and changed to be white. This method provides a representation of the

shape of the LOX-core with minimal influence from optical effects

4.1. Intact LOX-Core Length

The binary pictures allow clear definition of the dense LOX-core structure. Figure 8 presents the defined structures compared with corresponding OH* images. Near the injector head is an area with opaque expanded cold hydrogen which disturbs the detection of the LOX-jet. Downstream the LOX core is easily recognized. It can be clearly seen that the oxygen jet forms thread-like structures and downstream lumps break away which at high pressure are visible up to the end of the observation area.

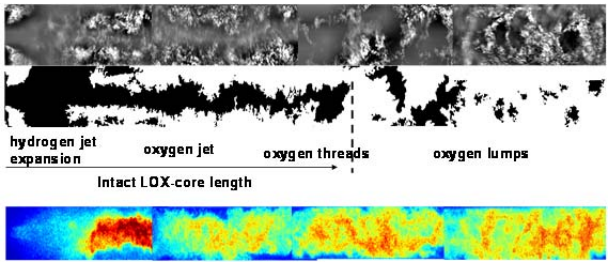

Figure 8: LOX-Core structure and corresponded OH images*

The analysis of the LOX jet structures delivers important information about the evolution of the jet, in particular at the location of the first interruption of the intact LOX-core. The distance between injection plane and this location is called intact LOX-core length in literature. Due to the dynamic character of the disintegration processes, an average value of this length typically has been taken into consideration. This parameter is strongly dependent on injector type as well operating conditions such as combustion chamber pressure and ROF (Figure 9, Figure 10).

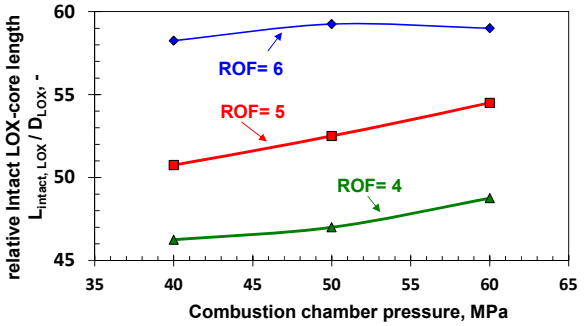

Figure 9: Intact LOX-core length as a function of combustion chamber pressure

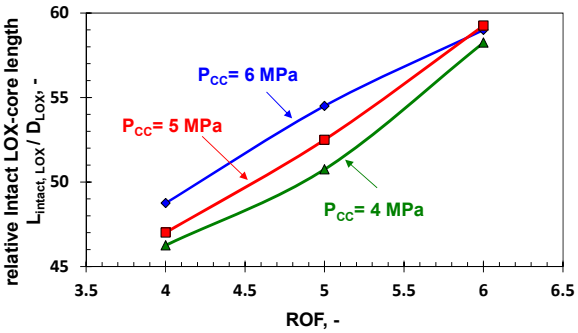

Figure 10: Intact LOX-core length as a function of oxygen-to-fuel ratio

Although the variance in intact core length also varies with operating condition, the figures present only time averaged values are presented.

Because the combustion chamber pressure and ratio of oxygen to fuel (ROF) were varied by changing of the mass flow rates, direct evaluation of the LOX-core lengths is difficult. For better comparison, Figure 11 and Figure 12 present the LOX-core length as a function of injection velocity ratio and momentum flux ratio. Due to the limited number of operating points and limited measurement accuracy, the results were approximated only by a linear function to show a tendency (Figure 11).

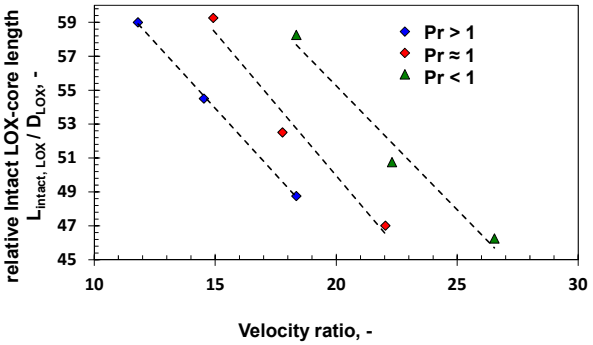

Figure 11: Intact LOX-core length as a function of velocity ratio

A direct comparison to results found in literature from investigations performed with substitute fluids (for example water or liquid nitrogen) is difficult because of the complex processes introduced by combustion of the cryogenic propellants. Only limited comparison will be made in this work.

In Figure 11, the relative intact core length is nearly proportional to velocity ratio with coefficient -1.57:

($L_{intact,LOX}/D_{LOX}$ ~ - 1.57*VR) and also shows a dependency on reduced pressure. In Figure 12, momentum flux ratio appears to adhere to the well know trend $L_{intact,LOX}/D_{LOX} \sim J^{-0.5}$ [10].

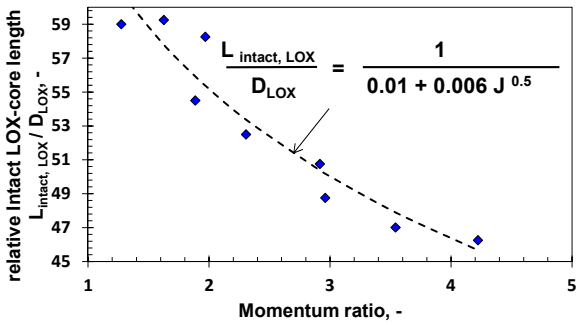

Figure 12: Intact LOX-core length as a function of momentum flux ratio

4.2. LOX-Core Velocity

Information on the velocity of the LOX-core can be obtained from time resolved observation of the location of the interruption of the LOX-core. A linear evolution of the position indicates a nearly constant LOX-core velocity in this area (Figure 13).

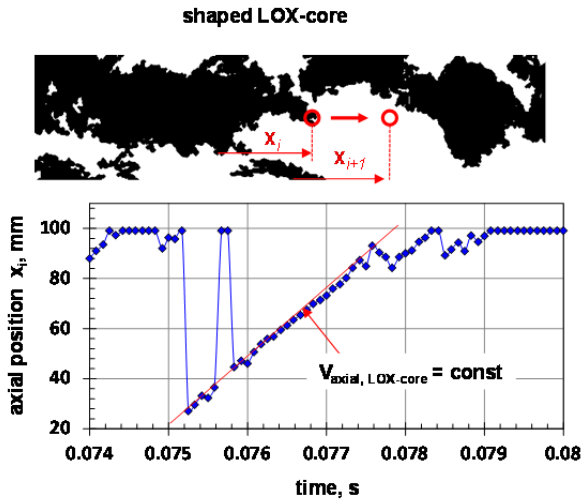

Figure 13: Definition of the LOX-core velocity using shadowgraph images

This method functions only by observation of the clearly visible position of first LOX-core interruption. Therefore it has been applied for configuration 2 at a mean observation position of x_{ref}= 140 mm and for configuration 3 at x_{ref}= 230 mm

Figure 14 shows the velocity at these two positions for different load points. The LOX-jet velocity increases with distance from the injection plane due to shear forces from H_2 annular jet as well as from surrounding hot gas flow which accelerates.

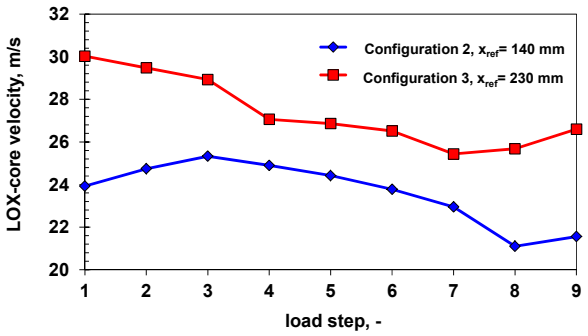

Figure 14: LOX-core velocity

4.3. LOX-Core Length

By analysis of LOX-core length it has been supposed that the visibility of the LOX-jet in shadowgraph images is primarily depended on the light refraction on the LOX-jet surface. Therefore it was assumed that in areas with high transmissivity and gradient variation (assigned as background, set to white) dense LOX-jet no longer exists. That does not necessarily mean that the oxygen concentration reaches zero in this area, but that high density, coherent LOX structures are missing. This assumption allows analysis of the LOX-core "full" disintegration length. For this purpose the binary (black-white) images have been additionally filtered to remove border effects. Areas with high absorption rate due to corner vortices on the edging of the glass windows have been suppressed.

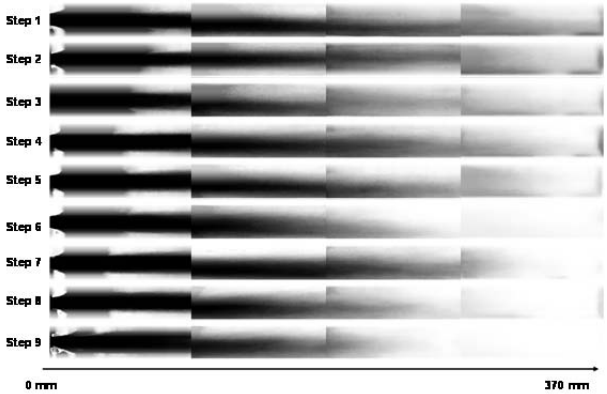

Figure 15: Compiled shadowgraph averaged images at different load steps

The processed images have then been composed to shape an average distribution of the

transparency for each load step (Figure 15). The relative integrated value of the absorption ratio permits conclusions to be drawn about the LOX-jet evolution. Figure 16 presents the distribution of the integral relative darkness as function of the distance from the injector head. A value of 1.0 corresponds to fully black and a value of 0.0 to fully white on a scale of grey values. LOX-core length is expected at a position where this distribution tends towards zero. The accumulated error due to the pre-processing and averaging operations significantly reduces measurement accuracy. Furthermore, the algorithm does not achieve complete suppression of the boundary effects at the ends of the windows, which leads to erroneous peaks at the transition between observation areas. However, this method suffices for determining the general trends.

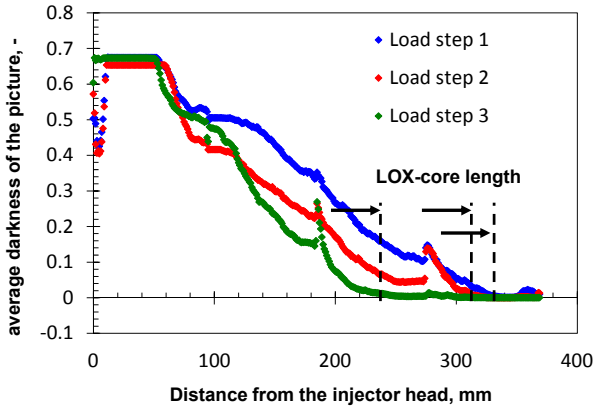

Figure 16: Distribution of the integral relative blackness along combustion chamber main axis

Similar to intact LOX-core length averaged from instantaneous measurements presented earlier (Figure 9, Figure 10), "full" LOX-core length shows obvious influence from combustion chamber pressure and mixture ratio (Figure 17, Figure 18).

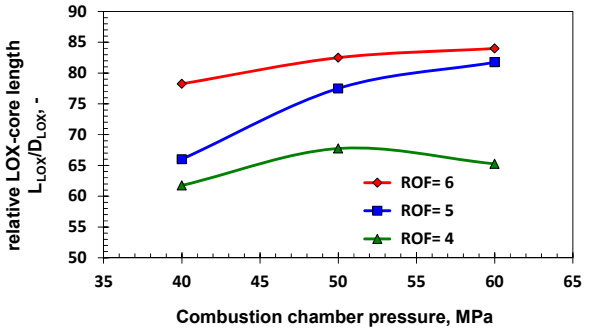

Figure 17: LOX-core length as a function of combustion chamber pressure

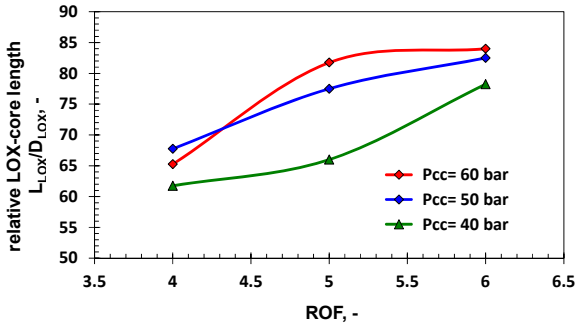

Figure 18: LOX-core length as a function of oxygen-to-fuel ratio

Dimensionless parameters velocity and momentum flux ratios were again used to analyze the trends. Figure 19 and Figure 20 present the LOX-core length as functions of corresponding injection velocity ratio and momentum flux ratio. Due to the relatively low accuracy the measurement results were approximated in both cases only by linear functions to show a tendency.

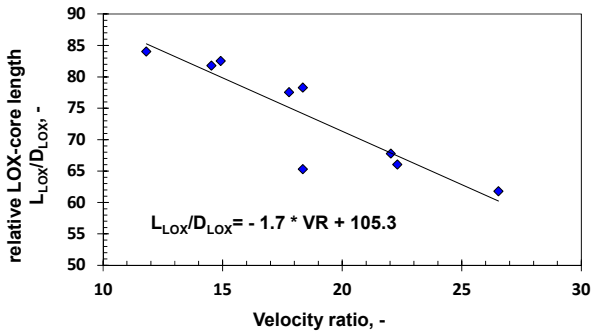

Figure 19: LOX-core length as a function from velocity ratio

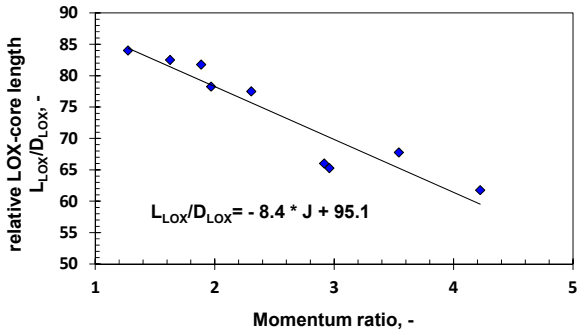

Figure 20: LOX-core length as a function from momentum ratio

5. CONCLUSION

Application of high-speed, time-resolved optical diagnostics in combination with conventional measurement techniques has provided quantitative and qualitative evidence of dissimilar combustion behavior at various reduced pressure levels through visualization and analysis of flow-field data. Such observations and results highlight the importance of further experimental investigations to provide additional fundamental information and enhance the current understanding of high-pressure, liquid rocket engine combustion. The data are expected to be of value in the validation of numerical tools for the design of liquid rocket engine thrust chambers.

6. REFERENCES

1. Haberzettl A. Gundel, D., Bahlmann K., ^ Oschwald, M., Kretschmer, J.,Thomas, J.L., Vuillermoz, P.,. European research and technology test bench P8 for high-pressure liquid rocket propellants. In: 36th AIAA/SAE/ASME/ASEE Joint Propulsion Conference, 2000
2. Locke J., Pal S, Woodward R., Santoro R, High Speed Visualization of LOX/GH2 Rocket Injector Flowfield: Hot-Fire and Cold-Flow Experiments, 46th AIAA/ASME/SAE/ASEE Joint Propulsion Conference & Exhibit, 2010
3. Lux, J., Suslov, D., Haidn, O., On porous liquid propellant rocket engine injectors, Aerospace Science and Technology, Vol. 12, No. 6, pp. 469-477, 2008
4. Mayer W. and Tamura H., Propellant Injection in a Liquid Oxygen/Gaseous Hydrogen Rocket Engine, Journal of Propulsion and Power. Vol. 12, No. 6, 1996, pp. 1137-1147.
5. Smith, J., Suslov, D., Langener , T., Oschwald, M., Schneider , G., Mayer, W., Hot-Fire testing of a LOX/H2 porous injector head at high pressure conditions with optical diagnostics, SPACE 2003, , 2003
6. Smith, J., Bechle, M., Suslov, D., Mayer, W., Oschwald, M., Haidn, O., Schneider, G., High pressure LOX/H2 combustion and flame dynamics, AIAA Paper, 40th AIAA/ASME/SAE/ASEE/ JPS Conference and Exhibit, 2004
7. Smith, J.J., Schneider, G.M., Suslov, D., Oschwald, M., Haidn, O. Steady-State, High Pressure LOx/H2 Rocket Engine Combustion, 1st European Conference for Aerospace Sciences, 2005
8. Suslov, D., Lux, J., Haidn, O., Investigation of porous injector elements for LOX/CH4 and LOX/H2 combustion at sub- and super-critical conditions, 2nd European Conference for Aerospace Sciences,2007
9. Suslov D., Hardi J., Knapp B., Oschwald M., Hot-fire testing of LOX/H2 single coaxial injector at high pressure conditions with optical diagnostics, 6th European Conference for Aeronautics and Space Sciences, 2015
10. Villermaux E., Mixing and Spray Formation in Coaxial Jets, Journal of Propulsion and Power, Vol. 14, No. 5, 1998